The Pennsylvania State University
Schreyer Honors College

Department of Biochemistry and Molecular Biology

LOCALIZATION OF PIP2 IN HGF-STIMULATED EPITHELIAL CELL MIGRATION AND INTEGRIN SIGNALING

AUSTIN BUSKIRK
SPRING 2024

A Thesis Submitted in Partial Fulfillment
of the Requirements
for a Baccalaureate Degree in Biochemistry
& Molecular Biology with honors in Biochemistry &
Molecular Biology

Reviewed and approved* by the following:

Lorraine Santy
Associate Professor of Biochemistry and Molecular Biology
Thesis Supervisor

Teh-hui Kao
Professor of Biochemistry & Molecular Biology
Honors Advisor

ABSTRACT

Epithelial cell migration is a physiological process that is important for the survival of many multicellular organisms. This process is critical for tissue renewal and repair as well as countless developmental components of various organisms. While the process of epithelial cell migration is critical for the survival of many organisms, disruption of epithelial cell migration can prove to be a prominent component of many diseases, including metastatic cancer and fibrosis. Due to the results of previously completed research, it is theorized that a phospholipid, phosphatidylinositol 4,5-bisphosphate (PIP2), binds other proteins to facilitate integrin recycling. As such, it can be suggested that PIP2 is a central component in integrin recycling and epithelial cell migration. This study was designed to study the localization and importance of PIP2 during integrin recycling. Adhesion assays conducted on HeLa cells, a cervical cell cancer line, were designed to study the impact of PIP2 in different endosomal compartments within HeLa cells, such as Rab7, Rab8, and Rab11. This was done by recruiting an enzyme capable of inactivating PIP2 to the varying endosomal compartments of interest and then quantifying the ability of the cells to adhere by using an adhesion assay in coordination with atomic absorption spectroscopy. The results indicate that PIP2 presence within the endosomal recycling pathway may have a significant impact on the ability of HeLa cells to recycle integrins.

TABLE OF CONTENTS

LIST OF FIGURES

LIST OF TABLES

ACKNOWLEDGEMENTS

There are several individuals I would like to thank for their continued assistance and support throughout my academic journey. First and foremost, I would like to thank Dr. Santy for her continuous support and encouragement throughout both my academic journey and thesis writing journey. She allowed me to pursue research, and she helped to foster my intrigue and desire to learn throughout the process. She allowed me to grow as an academic by providing me with critical support and wisdom throughout my research and academic endeavors. Dr. Santy truly helped me discover my passion for science.

I would also like to thank Kailee Jump, Ellen Lee, and Emma Huryn for their support and assistance over the course of the past few years. The insight and experience that each of them provided me with has helped me to develop my thesis and technical laboratory skills over the years.

Additionally, I would like to thank my advisors within the department of Biochemistry and Molecular Biology — Jennifer Keefer and Dr. Teh-hui Kao. I greatly appreciate your assistance and guidance throughout the past four years and would like to thank you again for taking the time to speak with me over the course of the countless meetings I scheduled. I would also like to thank the Eberly College of Science for the funding received in support of undergraduate research.

Finally, I would like to take this opportunity to thank my parents, my little sister, and my friends for being the best support system for me over the years. Their constant support and encouragement motivated me to pursue my goals and aspirations.

Chapter 1

Introduction

Epithelial Cells

Epithelial tissues are made of various cells, including cells that are cuboidal, columnar, and squamous cells (Nelson, 2009). When these cells form adhesions to their boundaries, they often take on an appearance that can best be described as a fried egg. While the individual structures of these cells are nothing astonishing, they can come together to form epithelial tissue — a complex netting of sorts that surrounds various organs or cavities throughout the body (Wang *et al.,* 2020).

Figure 1. Depiction of Epithelial Cell

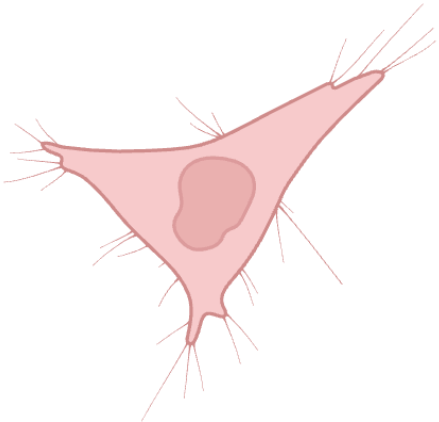

Figure 1 | *Depiction of Epithelial Cell.* The image above is a depiction of what the structure of epithelial cells can look like when adhered to a surface. These epithelial cells are specifically from that of a HeLa cell line typically have a structure like that of a fried egg when they are adhered to a surface due to adhesions stretching the cells apart. Image obtained from BioRender.com.

Epithelial cells line the outside of organs and blood vessels and compartmentalize the body cavities within animals. The cells can form a complex monolayer where the cells can form connections to one another that hold the cells in place. This monolayer structure can best be seen in *Figure 2*. Epithelial tissue sits on top of the basal surface — a semipermeable scaffolding of proteins that functions as a barrier between epithelial cells and the surrounding tissues. The basal surface defines the external barrier of various organs and lays the groundwork for epithelial cells to grow on. The cells also form various forms of cell-to-cell junctions that further lock the individual cells in place (Adil *et al.*, 2020).

Figure 2. Depiction of Epithelial Cell Monolayer

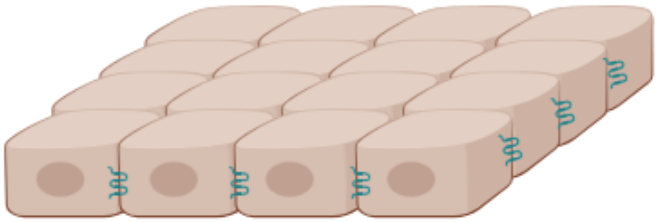

Figure 2 | *Depiction of Epithelial Cell Monolayer.* The image above is a depiction of what an epithelial cell monolayer can look like when cells are adhered to one another to form a boundary on top of the extracellular matrix (not shown). This figure specifically depicts a simple cuboidal monolayer, which is often used for passage of biomolecules in and out of organ systems. Intracellular connections between the epithelial cell are depicted in blue. Image obtained from BioRender.com.

Epithelial cells are stationary; however, migration of epithelial cells can be induced by various molecular pathways that can lead to epithelial cells becoming motile — one example of such is termed Epithelial-Mesenchymal Transition. Epithelial-Mesenchymal Transition is a phenomena that is vital for developmental processes and tissue repair (Yang & Weinberg, 2008).

Epithelial Cell Migration and Epithelial-Mesenchymal Transition

As previously aforementioned, the vast majority of epithelial cells present within an organism are stationary within the organism's body. However, epithelial-mesenchymal transition enables epithelial cells that were previously stationary to exhibit a phenotype that is similar to mesenchymal cells (Kalluri & Weinberg, 2009). These epithelial cells typically demonstrate a loss of polarity, decreased tight junction assembly, and often result in increased motility (Yang & Weinberg, 2008). This process is remarkably useful in developmental processes such as mesoderm and secondary palate formation but can lead to very harmful complications when the process becomes dysregulated in disease (Yang & Weinberg, 2008).

As previously mentioned, epithelial cells typically demonstrate a polarity that helps for the cells to determine in which direction they migrate (Yang & Weinberg, 2008). However, in cells that undergo epithelial mesenchymal transition, this polarity is often lost, which can result in unregulated localization of subcomponents of the cells, as well as the cells themselves. Of particular relevance to this study is the dysregulation of phosphatidylinositides once polarity is lost during epithelial mesenchymal transition. PIP2 is particularly interesting as it has been shown that it plays an important in generating asymmetry that is required for function in other cell types (Nelson, 2009).

While the vast majority of my research was directed towards understanding a subcomponent of the biochemical processes that govern epithelial cell migration induced by epithelial-mesenchymal transition, it is important to note that epithelial-mesenchymal transition also allows epithelial cells to exhibit a greater resistance to apoptosis and increased production of components of the extracellular matrix (Kalluri & Weinberg, 2009).

During the transition to a migratory phenotype, epithelial cells often exhibit a decrease in the production of molecules that typically adhere phenotypically normal cells in place

(Loh *et al.,* 2019). Two of these molecules are E-cadherin and N-cadherin. These cadherins also are components of various cellular signaling pathways that can be altered in Epithelial Mesenchymal Transition. Another molecule that is vital for both signaling pathways and adhesion within epithelial cells are integrins.

Figure 3. Epithelial-Mesenchymal Transition

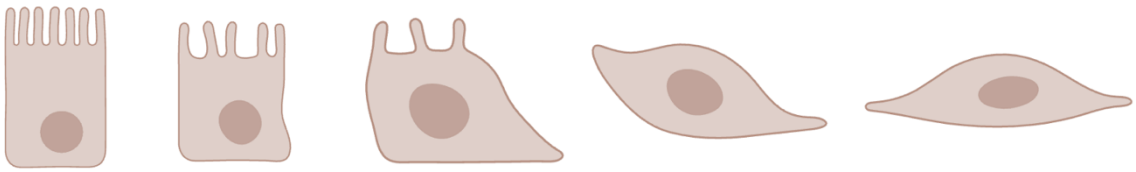

Figure 3 | *Epithelial-Mesenchymal Transition.* The figure above is a depiction of the progression of epithelial cells through Epithelial-Mesenchymal Transition. The cells begin differentiated and stationary. Once Epithelial-Mesenchymal Transition begins, the cell becomes less differentiated and begins to become more motile. Image obtained from BioRender.com.

Epithelial-mesenchymal transition is a unique phenomenon that dramatically alters the activity of cells with a wide range of functionality. Epithelial mesenchymal transition can be stimulated through a variety of growth factors, with the most common ones being hepatocyte growth factor (HGF), EGF, PDGF, and TGF-Beta (Kalluri & Weinberg, 2009). All of these growth factors have been linked to being responsible for the induction of epithelial mesenchymal transition.

Integrins

Integrins are transmembrane proteins that are vital for binding cells to the extracellular matrix. Integrins are typically homologous in nature and can play critical roles in various signal cascades within epithelial cells (Johnson & Lewis, 2002). Integrins contain alpha and beta strands. In focal adhesions, these strands coordinate the proteins present in the extracellular matrix on the outside of the cell with cytoskeleton on the inside of the cell. These focal adhesions function as both an anchor and a region for signaling in response to external stimuli (Hamidi & Ivaska, 2018). A structure of integrins and an example of signal transduction processes that they can be involved in are found in *Figure 4.*

Figure 4. Integrin Structure and Signal Cascade

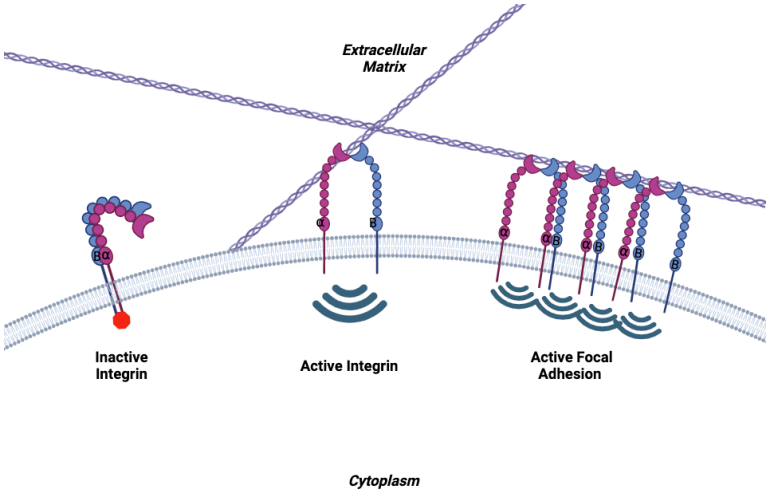

Figure 4 | *Integrin Structure and Signal Cascade.* The figure above depicts an integrin in both an active and inactive confirmation, as well as a cluster of integrins forming a focal adhesion. The Alpha and Beta strands bind ligands of interest — the extracellular matrix in this example — which induces a conformational change within the integrins that allows the downstream signal cascade to progress. Disruption in integrin recycling can impede associated signaling cascades as

well as cells ability to adhere, as in an adhesion assay (Hamidi & Ivaska, 2018). Image obtained from BioRender.com.

Another unique property of integrins and focal adhesions are that they play a critical role in the migration of cells. When cells need to move to one location to the other, they have to generate a propulsive force while migrating. Due to the fact that integrins connect the extracellular matrix to the cytoskeleton, integrins serve a critical role throughout the process as both traction sites for the epithelial cells but also as signal transducers that respond to mechanical stimulation (Ridley *et al*., 2003). While integrins in general are critical to directional migratory phenomena, focal adhesions — or clusters of integrins — are responsible for providing a traction point from which propulsive forces can originate (Ridley *et al*., 2003).

As epithelial cells move, the old focal adhesions begin to detach and new focal adhesions on the leading edge are formed that provide a new traction point from which propulsive forces are generated. As the cells move, old focal adhesions are endocytosed to remove the anchors that hold the cell in its current location, while kinesins can help to direct the endocytosed integrins (De Franceschi *et al*., 2015). In the process of focal adhesion formation on the cell's leading edge, integrins exocytosis towards the cell surface is signaled by various growth factors. As such, signal transduction pertaining to the exocytosis and recycling of integrins can profoundly affect the migration of epithelial cells and their ability to anchor in place.

As mentioned above, integrins play a critical role in the binding of cells to the extracellular matrix. In certain phenomena, such as metastasis, integrin function can be limited or impaired (Thapa & Anderson, 2012). The loss of phenotypically normal function of integrins can result from mutations in the protein structure of integrins. Another mechanism that can result in altered integrin function is mutation or variation in the focal adhesion turnover process. There are numerous mechanisms and signaling pathways that contribute to the regulation of integrin recycling. One such signaling molecule is phosphatidylinositol-4,5-biphosphate (PIP2).

Phosphatidylinositol-4,5-biphosphate (PIP2)

Phosphatidylinositol-4,5-biphosphate (PIP2) is a phosphoinositide. Similar to other phosphoinositides, it plays a major role in various cellular processes (Mandal, 2020). PIP2 levels can fluctuate at times and are regulated by phosphoinositide kinases and phosphatases. PIP2 can impact different processes through different phenomena such as by functioning as a binding site that other proteins can bind to or by stabilizing phosphoinositide pools in different endosomal compartments within the cell (Mandal, 2020). It is believed that PIP2's predominant function within the process of integrin recycling is to recruit other proteins critical to integrin recycling to the endosomal compartments when necessary. A structure of PIP2 can be found in *Figure 5*.

Figure 5. Phosphatidylinositol-4,5-biphosphate (PIP2)

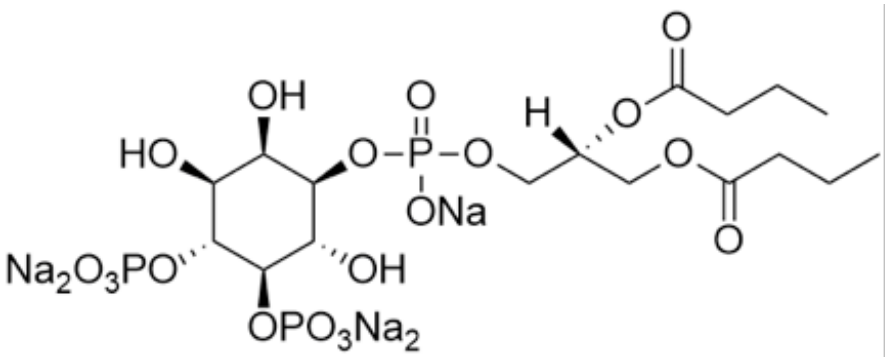

Figure 5 | *Phosphatidylinositol-4,5-biphosphate (PIP2).* The figure above is a depiction of the structure of Phosphatidylinositol-4,5-biphosphate (PIP2). This figure was obtained from Echelon Sciences.

PIP2 Role in Epithelial Cell Migration

PIP2 is a major component within various pathways that impact cellular dynamics and important processes within organisms. As previously mentioned, cellular adhesion is critical for different processes such as wound repair, and disrupted cellular adhesion can lead to various diseases, or potentially result in tumor metastasis. PIP2 plays a few different roles in the regulation and activity of integrin recycling and focal adhesion turnover.

PIP2 has the ability to bind and help mediate the activity of FAKs — focal adhesion kinases. When a cell is beginning the process of adhering to the extracellular matrix, FAKs are recruited to the cellular membrane at the site of different focal adhesion sites (Mandal, 2020). At these sites, FAKs must undergo a conformational change in order to begin the process of focal adhesion stimulation. As such, PIP2 plays an important role as a mediator molecule in the FAK dependent focal adhesion renewal process (Mandal, 2020).

Another way that PIP2 can promote adhesion is by binding and recruiting talin to the site of integrin recycling on the cellular membrane. Talin is traditionally in an inactive conformational state while in the cytosol. However, when talin interacts with PIP2 via a fluorescence resonance energy transfer (FRET), talin enters a different conformational state where it then becomes activated (Das *et al.*, 2014). Activated and membrane bound talin can then proceed to recruit vinculin. Vinuclin then plays a key role in the mediation of the interactions between actin and talin, which are critical for the renewal process of focal adhesions and integrins (Humphries *et al*., 2007).

While all of these different pathways involving PIP2 play a role in the process of integrin recycling, the pathway that is of particular interest is a result of pleckstrin homology domains (PH domains) and their interactions with phosphoinositides. While the specific interactions between PIPs and PH domains are widely unclear, it is understood that there are distinct structural

differences that lead certain proteins to associate with certain PIPs and not others (Singh *et al*., 2021). PH domains on proteins bind phosphoinositides; however, different PH domains can bind PIPs with different binding affinities (Oh & Santy, 2010). For example, a PH domain on one protein could bind certain alignments of PIP2, some will bind PIP2 and PIP3, and some will only bind PIP2. As such, there exists an array of PH domains that PIP2 is able to bind and recruit, which allows PIP2 to recruit certain proteins with the proper PH domain to its location. Studies show that cytohesins that have a PH domain that can bind to PIP2 are responsible for progression through integrin recycling (Oh & Santy, 2012).

PIP2 Localization in Epithelial Cell Migration

As can clearly be concluded from above, PIP2 is a crucial component of integrin recycling and focal adhesion reconstruction. The activity of PIP2 is wildly dependent on its location and its ability to bind and induce conformational changes in proteins in order to result in a physiological or molecular response that can be detected. While PIP2 is traditionally localized to the plasma membrane, it can be found throughout the cell throughout different endosomal compartments at different stages. While understanding this is important information, it is also important to understand where within the cells PIP2 is located where it is having the greatest impact on the ability of cells to recycle integrins. Understanding both the where, the when, and the how can help us to develop potential targets for therapeutic agents to combat different ailments that result from non-physiologically typical activity.

The Endosomal System

While the majority of PIP2 is found at the plasma membrane, it can be found throughout various different endosomal compartments during endocytosis. During the process of endocytosis, the invagination of the cellular membrane can cause PIP2 to be found within the various compartments that are created during endocytosis. Once the cellular membrane cleaves off and becomes its own vesicle, its location and final destination are in part controlled by Rab GTPases. There are different Rab GTPases that can signal for different vesicles to be localized at different locations. Rab GTPases often work by recruiting different effectors and regulators that help them to preferentially associate with intracellular compartment (Martínez-Arroyo *et al.*, 2021). Rab GTPases help to give the cellular membrane a sense of "identity" (Zerial & McBride, 2001). Because Rabs are specific to certain endosomal compartments, we can use their specificity to our advantage. The endosomal system and Rab specificity can be seen in *Figure 6.*

Figure 6. Rab Markers and the Endosomal System

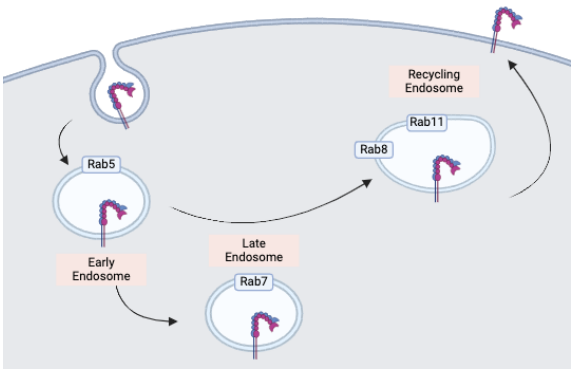

Figure 6 | ***Rab Markers and the Endosomal System.*** The figure above is a depiction of the endosomal system with a few of the endosomal compartments and the Rab GTPases associated with that compartment. Image obtained from BioRender.com.

In order to make use of the specificity that Rab GTPases offer, a synthetic Rab with an FRB tag was developed and transfected into the cells. In addition to the synthetically tagged Rab, a synthetic PseudoJanin that was tagged with an FKBP was also transfected into the cells. PseudoJanin is a synthetic enzyme that has two phosphatase domains that are capable of removing both phosphates from PIP2. In the presence of Rapamycin, the PseudoJanin would dimerize with the tagged Rab, thus recruiting the PseudoJanin to the associated endosomal compartment. PseudoJanin that is active has phosphatase domains that remove the phosphates from PIP2 which functionally inactivates the PIP2 within that endosomal compartment. This process is explained in more detail within *Chapter 2,* and contains *Figure 9*, which depicts the dimerization process.

Due to the fact that these various endosomal compartments can contain PIP2, it is worth delving deeper into the question of which of these endosomal compartments has the most PIP2, or has the PIP2 that is the most active in the integrin recycling pathway. A few Rab GTPases of interest and the compartment that they are associated with are found in *Table 1.*

Table 1. Endosomal Compartments and Associated Rab Markers

Endosomal Compartment	Associated Rab Markers
Late endosome	Rab7
Recycling Endosome	Rab8
Recycling Endosomes and Trans-Golgi Network	Rab11

Table 1 | *Endosomal Compartments and Associated Rab Markers.* The figure above lists certain endosomal compartments of interest within the endosomal system and the Rab GTPases that are associated with each endosomal compartment.

Experimental Objective and Research Question

As a result of the role that PIP2 plays in the process of integrin recycling, we decided to pursue research to determine the importance of PIP2 in integrin recycling. As such, the main goal of this experimental outline was to shine light on the process of integrin recycling by determining within what endosomal compartment PIP2 is required for integrin recycling. This was done by depleting PIP2 in endosomal compartments and checking to see if any of the endosomal compartments with depleted PIP2 exhibited impaired adhesion capabilities.

In order to help determine which endosomal compartments may contain PIP2 that is vital to the process of integrin recycling, a protocol was developed to study the effects of what the degradation of certain endosomal compartments — and therefor PIP2 —had on the ability for epithelial cells to recycle their integrins. This was done by degrading three separate endosomal compartments: Rab7, Rab8, and Rab11 and by then completing an adhesion assay to quantitatively analyze the degree with which epithelial cells were able to adhere to an extracellular matrix. It was hypothesized that epithelial cells who had PIP2 inactivated in relevant endosomal compartments would have the most impaired ability to adhere to the extracellular matrix in the adhesion assay.

Chapter 2

Materials and Methods

HeLa Cell Line

HeLa Cells were cultured in a media that includes 10% fetal bovine serum (FBS), 1% penicillin-streptomycin-fungizone, and 1% L-glutamine. The plated HeLa cells are incubated at 37°C in 5% CO2 in varying confluency. Cell lines are continuously split to reach a maximum confluence of 75%.

Cell Line Transfection

3 x 10^5 HeLa Cells are plated in a 6 cm tissue culture plate. The cells are incubated at 37°C overnight to reach optimal confluency in time for the transfection. Cells are transfected with DNA coding for Rab GTPases (FRB-tagged Rab) as well as an active or inactive PseudoJanin (FKBP-tagged PseudoJanin). The cells were transfected with 2 µg of each DNA coding sequence (the selected Rab GTPase and either an active PseudoJanin or an inactive PseudoJanin — which is the negative control), 500 µL of jetOPTIMUS® buffer, and 4 µL of jetOPTIMUS® reagent. The transfection solution incubated for 15 minutes at 22˚C. The transfection solution was added to the cells and the cells were incubated at 37°C overnight following the transfection protocol.

Adhesion Assay and Staining

Two days following the transfection of the HeLa cells, the cells are lifted using EDTA to chelate coordinating ions present within the integrins. The cells are allowed to incubate for 30 minutes at 22˚C. Once the incubation period has passed, the cells are counted and diluted to a concentration of 5 x 10^5 cells/mL. 100 µL of the cell suspension are placed into a row of wells with a gradient of fibronectin concentrations —1 µg/mL, 3 µg/mL, 5 µg/mL, and 10 µg/mL. This layout can better be understand by referencing the *96-well Plate Layout* figure.

Figure 7. Fibronectin Concentration Gradient

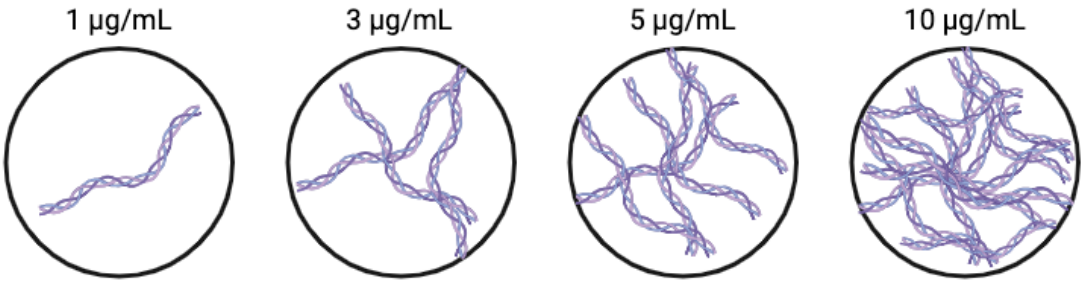

Figure 7 | *Fibronectin Concentration Gradient.* The figure above is a depiction of the concentration gradient of fibronectin used in the trial. Each glycogen chain is equivalent to 1 µg/mL of fibronectin used in the trial. The fibronectin network is designed to mimic the structure of the extracellular matrix. The more extracellular matrix — or fibronectin — present, the more opportunity there is for an epithelial cell to adhere to the structure. Image obtained from BioRender.com.

Figure 8. 96-well Plate Layout

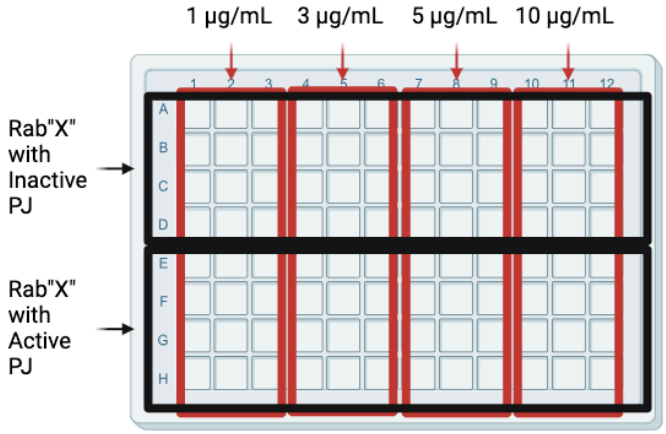

Figure 8 | *96-well Plate Layout.* The figure above is a depiction of the standard layout that was utilized when conducting trials. Image obtained from BioRender.com.

Each well also has 50 µL of 0.2% HI-BSA. The cells are allowed to incubate for 45 minutes at 22℃. Following the incubation time frame, the Cells were rinsed with 1X phosphate-buffered saline (PBS). The wells with cells were then fixed with 50 µl of 4% paraformaldehyde (0.1 M sodium phosphate buffer, pH 7.3) for 15 minutes at 22°C room temperature. Cells were rinsed twice with 1X PBS. 50 µL of Crystal Violet is added to each well and allowed to incubate for 15 minutes at 22℃. The cells are then rinsed with distilled water repeatedly until the runoff runs clear. 150 µL of 1.0% Deoxycholate is then added and allowed to incubate for 15 minutes at 22℃. The 96 well plate is then run through an atomic absorbance reader for a wavelength of 595 nm. The crystal violet functions as a total protein stain, so by utilizing the stain and quantifying the amount of crystal violate left through an OD 595 nm reading, we can relate the total amount of crystal violet remaining through the absorbance reading to the total amount of cells left, as total protein content and number of cells are proportional to one another.

PseudoJanin Recruitment

As mentioned in the introduction of this paper, the HeLa cells are transfected with a Rab GTPase — which is FRB-tagged — as well as an active or inactive PseudoJanin — which is FKBP-tagged. Once the process of chelating the integrins with EDTA began, 5 µL — or a 1:1000 dilution — of Rapamycin (a dimerization drug) was added to the plate to cause the tagged Rab and tagged PseudoJanin to dimerize. Once the cells were adequately lifted, they were spun down and diluted into a volume of PBS that yielded a concentration of 5×10^5 cells/mL. A 1:1000 dilution of Rapamycin was once again added to this new volume to ensure that the dimerization process was able to reach completion. The process of dimerization and the interactions between the components of the dimerization process can be seen in more detail in the figure *Rab and PseudoJanin Dimerization.*

Figure 9. Rab and PseudoJanin Dimerization

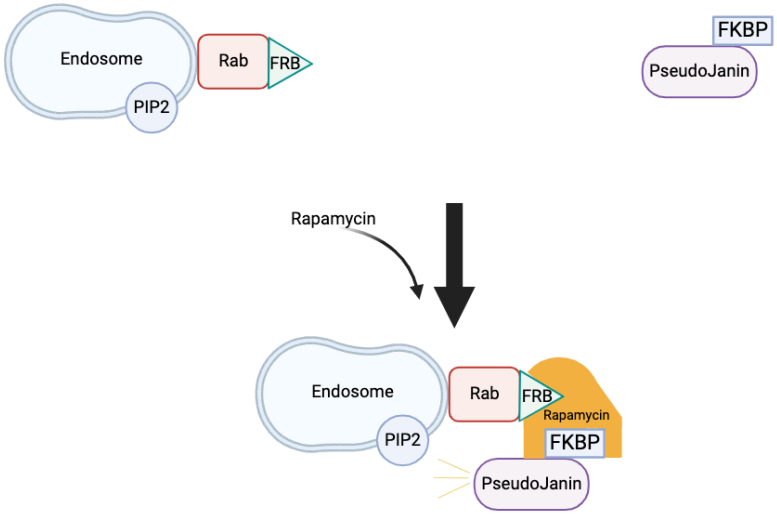

Figure 9 | *Rab and PseudoJanin Dimerization.* The figure above is a depiction of the dimerization of Rab and PseudoJanin.

When the Rapamycin is added, the tagged PseudoJanin and Rab dimerize. While the dimerization occurs, the PseudoJanin is recruited to the endosome (that the Rab is associated with) where it is now near the PIP2. If the PseudoJanin is catalytically active, it will remove a phosphate group from the PIP2, inactivating it and ceasing all downstream signals from the PIP2 it is within proximity of (Sohn *et al.*, 2018). By dimerizing an active PseudoJanin to the endosomal compartment associated with the Rab, the PIP2 within that compartment is effectively rendered inactive. As such, the PIP2 can't recruit proteins that stimulate the exit of integrins towards the cell surface.

Chapter 3

Results

As discussed in Chapter 1, PIP2 is an important mediator in the process of HGF stimulated epithelial cell migration. The ability of PIP2 to mediate such processes is dependent on its location, as are most proteins. While PIP2 is traditionally localized to the plasma membrane, it can be found throughout the cell and it can be located in various endosomal compartments within the epithelial cells. In order to research which of the endosomal compartments PIP2 presence may be most important in — with respect to integrin recycling — an adhesion assay was performed to test what the impact of inactivating PIP2 within different endosomal compartments would have on integrin and focal adhesion renewal. Endosomal compartments with Rab7, Rab8, and Rab 11 protein markers that recruited PseudoJanin to the endosomal compartment that could cleave a phosphate on PIP2, thus inactivating it and it's downstream effects.

For each trial, only one endosomal marker was tested, with the goal being to compare the sample with an endosomal compartment with inactivated PIP2 with a trial that had not had PIP2 inactivated. In order to achieve this, epithelial cells were transfected with synthetic Rab analogs as well as PseudoJanin or PseudoJanin Dead. The Rab analogs were designed so that they could dimerize with PseudoJanin in the presence of a dimerization drug. PseudoJanin Dead (or inactive PseudoJanin) did not have the catalytic activity to cleave a phosphate from PIP2. Endosomal compartments that contained the Rab protein markers that dimerized with active PseudoJanin had PIP2 within that compartment inactivated by the catalytically active PseudoJanin by removing a phosphate from PIP2. The integrins on the surface of the cells were destroyed by using EDTA, which removed the calcium ions present to denature the proteins (Lai *et al.*, 2022). The cells were then counted and the volume adjusted to reach a final concentration of 5×10^5 cells/mL. While 5

x 10^5 cells/mL was the intended concentration for each trial to be ran at, some trials were run at a lower concentration. In these instances, both the trials with the active PseudoJanin and inactive PseudoJanin were run at adjusted concentrations when cell confluence didn't permit a concentration of 5 x 10^5 cells/mL. Utilizing the adhesion assay methodology discussed in Chapter 2 and the layout depicted in *96-well Layout* figure, the ability of the cells to adhere was quantitatively measured by measuring the optical density of each well at 595 nm.

The "raw data" for each trial is presented in the appendix for each trial. Utilizing the collected raw data, an average and standard deviation was calculated for each Rab and PseudoJanin combination for each concentration of fibronectin. Utilizing the averages from these charts, an average normalized absorbance was determined by dividing the average absorbance for each concentration of fibronectin for each trial by the average absorbance for the 1 μg/mL sample with inactive PseudoJanin. This was done to account for variability in experimental protocol. The normalized average absorbance for each sample was graphed, and a paired T-test completed to test for statistical significance.

It was hypothesized that the Rab protein marker that corresponded to the endosomal compartment that contained the PIP2 most vital for integrin recycling would demonstrate a decrease in absorbance as a result of impaired integrin recycling capabilities. The absorbance data for each sample with and without an active PseudoJanin was compared, and the effect of inactivation of PIP2 within these endosomal compartments was quantified through the change in absorbance. Furthermore, a few other hypotheses that were made in the process of optimizing the protocol were: 1) increasing the concentration of fibronectin would increase the amount of cells bound to the surface and thus increase the absorbance; 2) Destruction of an endosomal compartment would not increase the ability of cells to adhere in a statistically significant manner.

Control Results

Table 2. Summarization of Control Data

	1 (µg/mL)	3 (µg/mL)	5 (µg/mL)	10 (µg/mL)
AVERAGE ABSORBANCE	1.6892	1.7849	1.7631	1.8434
STANDARD DEVIATION	.816	.821	.867	.863

Table 2 | ***Summarization of Control Data.*** The table above contains the calculated average absorbance and standard deviation for the control data at a fibronectin concentration of 1 µg/mL, 3 µg/mL, 5 µg/mL, and 10 µg/mL. The average for each concentration was calculated by summating the absorbance of the raw data for the control trials at each concentration of fibronectin and then dividing it by the sample size. The raw data utilized to calculate these values can be found in the appendix.

Figure 10. Visualization of Control Data

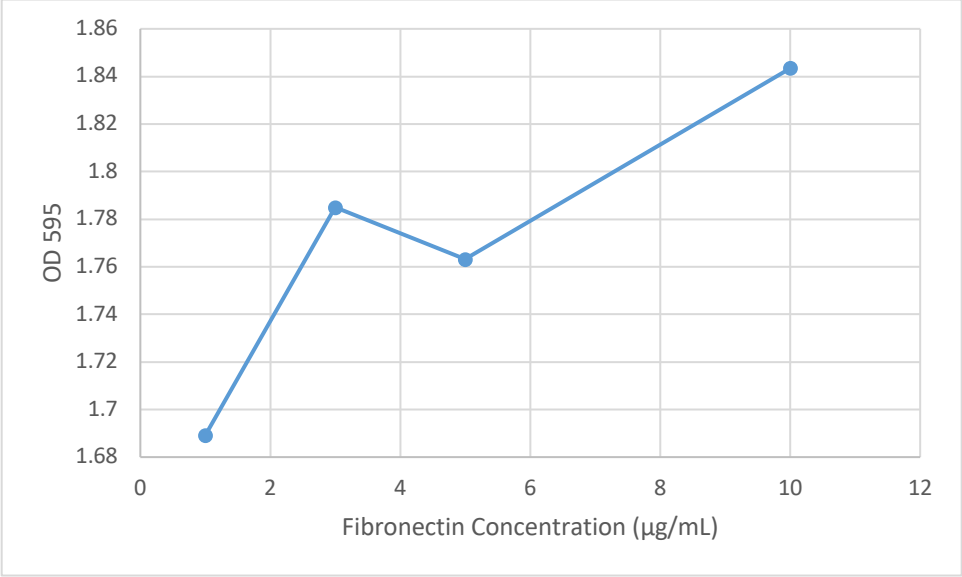

Figure 10 | ***Visualization of Control Data.*** The graph above depicts the calculated average absorbance for the control data in respect fibronectin concentration. Fibronectin concentrations of 1 µg/mL, 3 µg/mL, 5 µg/mL, and 10 µg/mL were measured.

Figure 11. Visualization of Control Data Variability

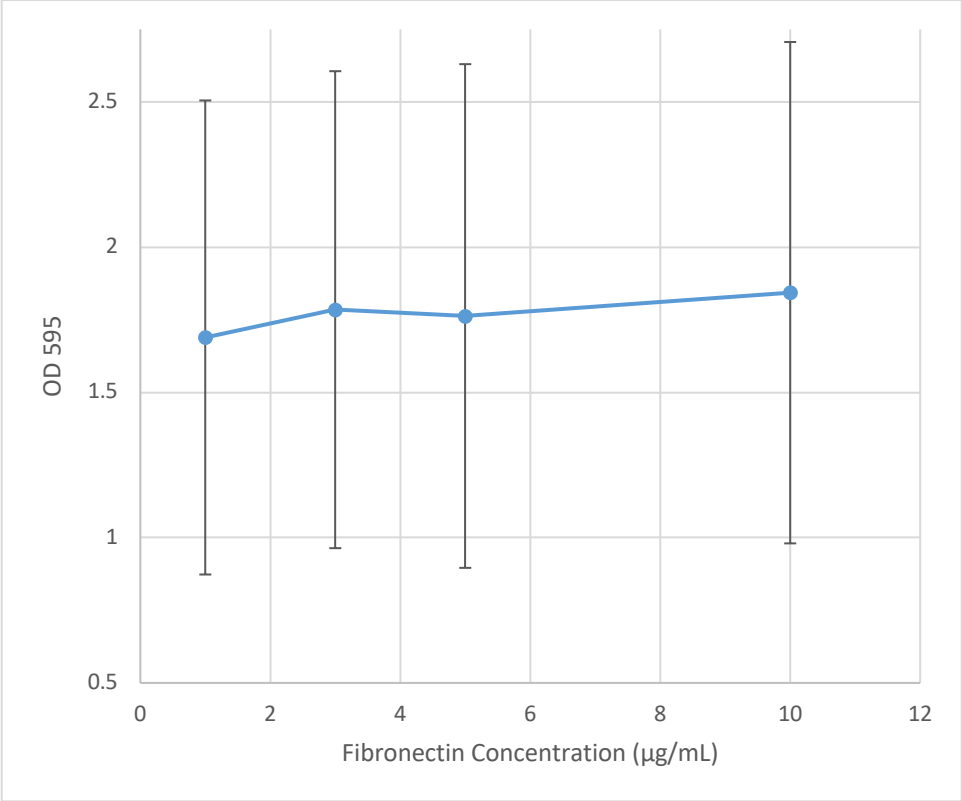

Figure 11| *Visualization of Control Data Variability.* The graph above depicts the calculated average absorbance for the control data in respect fibronectin concentration. Fibronectin concentrations of 1 µg/mL, 3 µg/mL, 5 µg/mL, and 10 µg/mL were measured. Additionally, the graph contains error bars that depict the standard deviation of each sample, which is present in *Summarization of Control Data*.

Table 3. Normalization of Control Data

	1 (µg/mL)	3 (µg/mL)	5 (µg/mL)	10 (µg/mL)
NORMALIZED AVERAGE ABSORBANCE	1	1.056	1.044	1.091
STANDARD DEVIATION	.48	.49	.51	.51

Table 3 | *Normalization of Control Data.* The table above contains the calculated normalized average absorbance and percent change in absorbance for each tested concentration of fibronectin. The normalized average absorbance was calculated by dividing the average absorbance of the 1 µg/mL, 3 µg/mL, 5 µg/mL, and 10 µg/mL sample by the average absorbance of the 1 µg/mL sample. The new normalized standard deviation was calculated by dividing the original calculated standard deviation for each trial by the the average absorbance of the 1 µg/mL sample

Figure 12. Visualization of Normalized Control Data

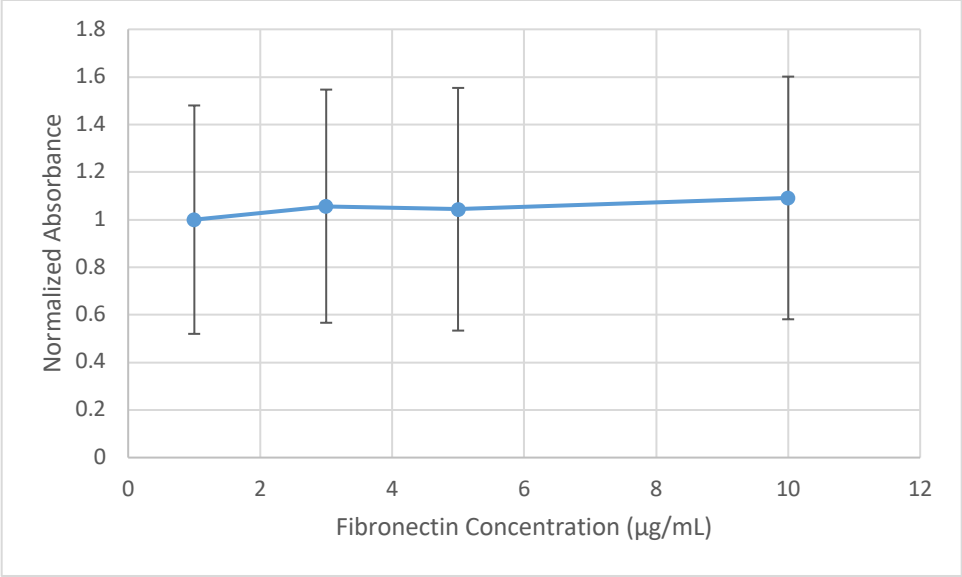

Figure 12 | *Visualization of Normalized Control Data.* The graph above depicts the calculated normalized average absorbance for the control data in respect fibronectin concentration. Fibronectin concentrations of 1 µg/mL, 3 µg/mL, 5 µg/mL, and 10 µg/mL were measured. Additionally, the graph contains error bars that depict the standard deviation of each sample, which is present in *Normalization of Control Data*.

Control Results Summary

As can be seen in *Visualization of Control Data,* the sample has a slight decrease in absorbance when going from 3 µg/mL to 5 µg/mL. This scientifically does not make sense, as increasing the amount of extracellular matrix should not results in a decrease in absorbance for the sample. Despite this, the data did have an upward trend of absorbance, going from a normalized average of 1 at 1 µg/mL to 1.091 at 10 µg/mL. The data does indicate there is a high degree of variability associated with OD 595 with respect to the adhesion assay and absorbance protocol.

Rab8 GTPase Results

Table 4. Summarization of Rab8 with Active PseudoJanin Data

	1 (µg/mL)	3 (µg/mL)	5 (µg/mL)	10 (µg/mL)
AVERAGE ABSORBANCE	1.377	1.448	1.524	1.670
STANDARD DEVIATION	.853	.943	.886	.886

Table 4 | ***Summarization of Rab8 with Active PseudoJanin Data.*** The table above contains the calculated average absorbance and standard deviation for the Rab8 trial that had active PseudoJanin at a fibronectin concentration of 1 µg/mL, 3 µg/mL, 5 µg/mL, and 10 µg/mL. The average for each concentration was calculated by summating the absorbance of the raw data for the Rab8 trials that had active PseudoJanin at each concentration of fibronectin and then dividing it by the sample size. The raw data utilized to calculate these values can be found in the appendix.

Table 5. Summarization of Rab8 with Inactive PseudoJanin Data

	1 (µg/mL)	3 (µg/mL)	5 (µg/mL)	10 (µg/mL)
AVERAGE ABSORBANCE	1.602	1.568	1.630	1.764
STANDARD DEVIATION	.942	1.035	.997	.935

Table 5 | ***Summarization of Rab8 with Inactive PseudoJanin Data.*** The table above contains the calculated average absorbance and standard deviation for the Rab8 trial that had inactive PseudoJanin at a fibronectin concentration of 1 µg/mL, 3 µg/mL, 5 µg/mL, and 10 µg/mL. The average for each concentration was calculated by summating the absorbance of the raw data for the Rab8 trials that had inactive PseudoJanin at each concentration of fibronectin and then dividing it by the sample size. The raw data utilized to calculate these values can be found in the appendix.

Table 6. Normalization of Rab8 with Active PseudoJanin Data

	1 (µg/mL)	3 (µg/mL)	5 (µg/mL)	10 (µg/mL)
NORMALIZED AVERAGE ABSORBANCE	.860	.904	.951	1.042
STANDARD DEVIATION	.53	.59	.55	.55

Table 6 | ***Normalization of Rab8 with Active PseudoJanin Data.*** The table above contains the calculated normalized average absorbance and percent change in absorbance for each tested concentration of fibronectin of the Rab8 sample with active PseudoJanin. The normalized average absorbance was calculated by dividing the average absorbance of the 1 µg/mL, 3 µg/mL, 5 µg/mL, and 10 µg/mL of the Rab8 with active PseudoJanin sample by the average absorbance of the 1 µg/mL sample of the Rab 8 with inactive PseudoJanin. The new normalized standard deviation was calculated by dividing the original calculated standard deviation for each trial — found in *Summarization of Rab8 with Active PseudoJanin Dat*a — by the average absorbance of the 1 µg/mL sample of the Rab 8 with inactive PseudoJanin

Table 7. Normalization of Rab8 with Inactive PseudoJanin Data

	1 (µg/mL)	3 (µg/mL)	5 (µg/mL)	10 (µg/mL)
AVERAGE ABSORBANCE	1	.978	1.017	1.101
STANDARD DEVIATION	.59	.65	.62	.58

Table 7 | ***Normalization of Rab8 with Inactive PseudoJanin Data.*** The table above contains the calculated normalized average absorbance and percent change in absorbance for each tested concentration of fibronectin of the Rab8 sample with inactive PseudoJanin. The normalized average absorbance was calculated by dividing the average absorbance of the 1 µg/mL, 3 µg/mL, 5 µg/mL, and 10 µg/mL of the Rab8 with inactive PseudoJanin sample by the average absorbance of the 1 µg/mL sample of the Rab 8 with inactive PseudoJanin. The new normalized standard deviation was calculated by dividing the original calculated standard deviation for each trial — found in *Summarization of Rab8 with Inactive PseudoJanin Dat*a — by the average absorbance of the 1 µg/mL sample of the Rab8 with inactive PseudoJanin.

Figure 13. Comparison of Normalized Rab8 Data with Active and Inactive PseudoJanin

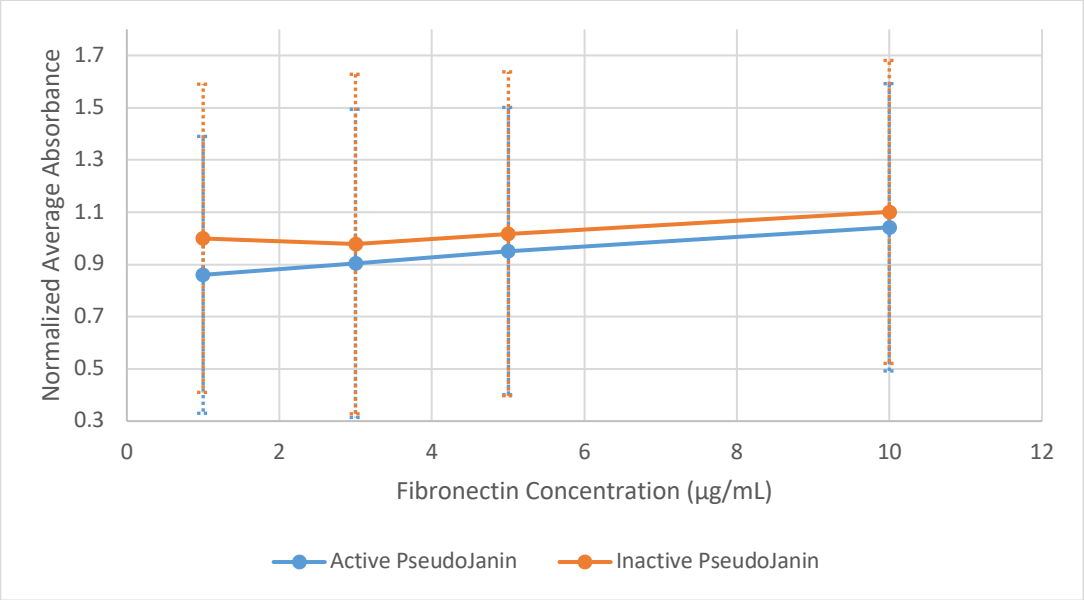

Figure 13 | ***Comparison of Normalized Absorbance Rab8 Data with Active and Inactive PseudoJanin.*** The graph above depicts the calculated normalized average absorbance for both the Rab8 trial that had an active PseudoJanin, as well as the trial that had an inactive PseudoJanin. The calculated normalized average absorbance for each trial was graphed in relation to the fibronectin concentrations (1 µg/mL, 3 µg/mL, 5 µg/mL, and 10 µg/mL) for which the data was measured. The error bars represent the standard deviation of each trial and are present within *Normalization of Rab8 with Inactive PseudoJanin Data* and *Normalization of Rab8 with Active PseudoJanin Data* tables.

Table 8. Paired T-Test of Rab8 Data

Fibronectin Concentration	Two-Tailed P Value
1 µg/mL	.2442
3 µg/mL	.5771
5 µg/mL	.5980
10 µg/mL	.6258

Table 8 | ***Paired T-Test of Rab8 Data.*** The table above includes the two-tailed P value calculated when comparing the normalized average absorbance data for the Rab8 trials with active and inactive PseudoJanin.

Rab8 Results Summary

As can be seen in the *Comparison of Normalized Average Absorbance of Rab8 with Active and Inactive PseudoJanin,* the Rab8 sample that had a phosphate group cleaved from PIP2, the sample with active PsuedoJanin, did exhibit a lower absorbance compared to the sample that did not have a phosphate group cleaved (Inactive PseudoJanin). The Rab8 sample with the inactive PseudoJanin had a larger normalized average absorbance than the Rab8 sample with the active PseudoJanin at each concentration of fibronectin.

While this trend was able to be observed, it is worth noting that there was no significant differences between the normalized average absorbance of the Rab8 samples. The paired T-test for the 1 μg/mL samples of Rab8 with and without an active PseudoJanin yielded a two-tailed P value of .2442, which is considered to be a statistically insignificant difference. The paired T-test for the 3 μg/mL samples of Rab8 with and without an active PseudoJanin yielded a two-tailed P value of .5771, which is considered to be a statistically insignificant difference. The paired T-test for the 5 μg/mL samples of Rab8 with and without an active PseudoJanin yielded a two-tailed P value of .5980, which is considered to be a statistically insignificant difference. The paired T-test for the 10 μg/mL samples of Rab8 with and without an active PseudoJanin yielded a two-tailed P value of .5980, which is considered to be a statistically insignificant difference.

Similar to the control data Inactive PseudoJanin sample again exhibits a decrease in absorbance, and there for a decrease binding capabilities when going from 1 μg/mL of fibronectin to 3 μg/mL of fibronectin. This does not scientifically make sense.

In addition to the deviation from the expected trends in the absorbance as concentration increased, the variability in the data, measured by standard deviation, of the Rab8 trials were concernedly large.

Rab7 GTPase Results

Table 9. Summarization of Rab7 with Active PseudoJanin Data

	1 (µg/mL)	3 (µg/mL)	5 (µg/mL)	10 (µg/mL)
AVERAGE ABSORBANCE	1.077	1.186	1.168	1.477
STANDARD DEVIATION	.688	.765	.812	.988

Table 9 | ***Summarization of Rab7 with Active PseudoJanin Data.*** The table above contains the calculated average absorbance and standard deviation for the Rab7 trial that had active PseudoJanin at a fibronectin concentration of 1 µg/mL, 3 µg/mL, 5 µg/mL, and 10 µg/mL. The average for each concentration was calculated by summating the absorbance of the raw data for the Rab7 trials that had active PseudoJanin at each concentration of fibronectin and then dividing it by the sample size.

Table 10. Summarization of Rab7 with Inactive PseudoJanin Data

	1 (µg/mL)	3 (µg/mL)	5 (µg/mL)	10 (µg/mL)
AVERAGE ABSORBANCE	1.184	1.180	1.391	1.467
STANDARD DEVIATION	.823	.686	1.012	.916

Table 10 | ***Summarization of Rab7 with Inactive PseudoJanin Data.*** The table above contains the calculated average absorbance and standard deviation for the Rab7 trial that had inactive PseudoJanin at a fibronectin concentration of 1 µg/mL, 3 µg/mL, 5 µg/mL, and 10 µg/mL. The average for each concentration was calculated by summating the absorbance of the raw data for the Rab7 trials that had inactive PseudoJanin at each concentration of fibronectin and then dividing it by the sample size.

Table 11. Normalization of Rab7 with Active PseudoJanin Data

	1 (µg/mL)	3 (µg/mL)	5 (µg/mL)	10 (µg/mL)
NORMALIZED AVERAGE ABSORBANCE	.910	1.002	.986	1.247
STANDARD DEVIATION	.58	.65	.68	1.08

Table 11 | ***Normalization of Rab7 with Active PseudoJanin Data.*** The table above contains the calculated normalized average absorbance and percent change in absorbance for each tested concentration of fibronectin of the Rab7 sample with active PseudoJanin. The normalized average absorbance was calculated by dividing the average absorbance of the 1 µg/mL, 3 µg/mL, 5 µg/mL, and 10 µg/mL of the Rab7 with active PseudoJanin sample by the average absorbance of the 1 µg/mL sample of the Rab7 with inactive PseudoJanin. The new normalized standard deviation was calculated by dividing the original calculated standard deviation for each trial — found in *Summarization of Rab7 with Active PseudoJanin Data* — by the average absorbance of the 1 µg/mL sample of the Rab7 with inactive PseudoJanin

Table 12. Normalization of Rab7 with Inactive PseudoJanin Data

	1 (µg/mL)	3 (µg/mL)	5 (µg/mL)	10 (µg/mL)
AVERAGE ABSORBANCE	1	.997	1.175	1.240
STANDARD DEVIATION	.70	.58	.86	.77

Table 12 | ***Normalization of Rab7 with Inactive PseudoJanin Data.*** The table above contains the calculated normalized average absorbance and percent change in absorbance for each tested concentration of fibronectin of the Rab7 sample with inactive PseudoJanin. The normalized average absorbance was calculated by dividing the average absorbance of the 1 µg/mL, 3 µg/mL, 5 µg/mL, and 10 µg/mL of the Rab7 with inactive PseudoJanin sample by the average absorbance of the 1 µg/mL sample of the Rab 7 with inactive PseudoJanin. The new normalized standard deviation was calculated by dividing the original calculated standard deviation for each trial — found in *Summarization of Rab7 with Inactive PseudoJanin Data* — by the average absorbance of the 1 µg/mL sample of the Rab7 with inactive PseudoJanin.

Figure 14. Comparison of Normalized Rab7 Data with Active and Inactive PseudoJanin

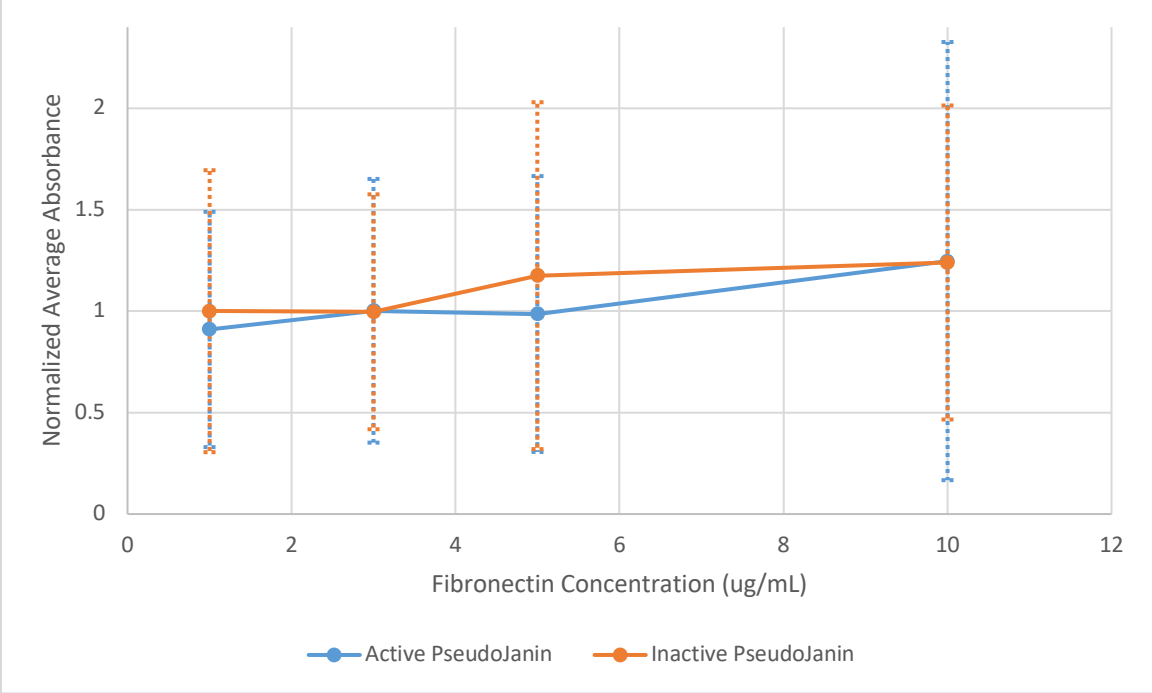

Figure 14 | ***Comparison of Normalized Rab7 Data with Active and Inactive PseudoJanin.*** The graph above depicts the calculated normalized average absorbance for both the Rab7 trial that had an active PseudoJanin, as well as the trial that had an inactive PseudoJanin. The calculated normalized average absorbance for each trial was graphed in relation to the fibronectin concentrations (1 µg/mL, 3 µg/mL, 5 µg/mL, and 10 µg/mL) for which the data was measured. The error bars represent the standard deviation of each trial and are present within *Normalization of Rab7 with Inactive PseudoJanin Data* and *Normalization of Rab7 with Active PseudoJanin Data* tables.

Table 13. Paired T-Test of Rab7 Data

Fibronectin Concentration	Two-Tailed P Value
1 µg/mL	.6758
3 µg/mL	.9807
5 µg/mL	.4680
10 µg/mL	.9823

Table 13 | ***Paired T-Test of Rab8 Data.*** The table above includes the two-tailed P value calculated when comparing the normalized absorbance data for the Rab7 trials with active and inactive PseudoJanin.

Rab7 Results Summary

As can be seen in the *Comparison of Normalized Average Absorbance of Rab7 with Active and Inactive PseudoJanin* and the sample that had a phosphate group removed from PIP2, the sample with active PsuedoJanin, and the sample that did not have a phosphate group removed from PIP2 (Inactive PseudoJanin), did not exhibit any detectable relationship in the obtained data. The Rab7 sample with the inactive PseudoJanin had a larger normalized average absorbance at 1 µg/mL and 3 µg/mL of fibronectin, while the Rab7 sample with the active PseudoJanin had a larger normalized average absorbance at 3 µg/mL and 10 µg/mL.

While a qualitative analysis of the graph may indicate that there was no significant trend detected in the trials, a statistical analysis indicates that there was no significant differences between the normalized average absorbance of the Rab7 samples. The paired T-test for the 1 µg/mL samples of Rab7 with and without an active PseudoJanin yielded a two-tailed P value of .6758, which is considered to be a statistically insignificant difference. The paired T-test for the 3 µg/mL samples of Rab7 with and without an active PseudoJanin yielded a two-tailed P value of .9807, which is considered to be a statistically insignificant difference. The paired T-test for the 5 µg/mL samples of Rab7 with and without an active PseudoJanin yielded a two-tailed P value of .4680, which is considered to be a statistically insignificant difference. The paired T-test for the 10 µg/mL samples of Rab7 with and without an active PseudoJanin yielded a two-tailed P value of .9823, which is considered to be a statistically insignificant difference.

Similar to the control, two samples exhibited a decrease in normalized average absorbance as the concentration of fibronectin increased. This does not scientifically make sense.

In addition to the deviation from the expected trends in the absorbance as concentration increased, the variability in the data, measured by standard deviation, of the Rab7 trials were large in respect to the other trials.

Rab11 GTPase Results

Table 14. Summarization of Rab11 with Active PseudoJanin Data

	1(µg/mL)	3 (µg/mL)	5 (µg/mL)	10 (µg/mL)
AVERAGE ABSORBANCE	1.142	1.155	1.307	1.469
STANDARD DEVIATION	.782	.786	.880	.916

Table 14 | ***Summarization of Rab11 with Active PseudoJanin Data.*** The table above contains the calculated average absorbance and standard deviation for the Rab11 trial that had active PseudoJanin at a fibronectin concentration of 1 µg/mL, 3 µg/mL, 5 µg/mL, and 10 µg/mL. The average for each concentration was calculated by summating the absorbance of the raw data for the Rab11 trials that had active PseudoJanin at each concentration of fibronectin and then dividing it by the sample size.

Table 15. Summarization of Rab11 with Inactive PseudoJanin Data

	1 (µg/mL)	3 (µg/mL)	5 (µg/mL)	10 (µg/mL)
AVERAGE ABSORBANCE	1.394	1.470	1.601	1.788
STANDARD DEVIATION	.757	.832	.872	.907

Table 15 | ***Summarization of Rab11 with Inactive PseudoJanin Data.*** The table above contains the calculated average absorbance and standard deviation for the Rab11 trial that had inactive PseudoJanin at a fibronectin concentration of 1 µg/mL, 3 µg/mL, 5 µg/mL, and 10 µg/mL. The average for each concentration was calculated by summating the absorbance of the raw data for the Rab11 trials that had inactive PseudoJanin at each concentration of fibronectin and then dividing it by the sample size.

Table 16. Normalization of Rab11 with Active PseudoJanin Data

	1 (µg/mL)	3 (µg/mL)	5 (µg/mL)	10 (µg/mL)
NORMALIZED AVERAGE ABSORBANCE	.819	.829	.938	1.054
STANDARD DEVIATION	.56	.56	.63	.66

Table 16 | ***Normalization of Rab11 with Active PseudoJanin Data.*** The table above contains the calculated normalized average absorbance and percent change in absorbance for each tested concentration of fibronectin of the Rab11 sample with active PseudoJanin. The normalized average absorbance was calculated by dividing the average absorbance of the 1 µg/mL, 3 µg/mL, 5 µg/mL, and 10 µg/mL of the Rab11 with active PseudoJanin sample by the average absorbance of the 1 µg/mL sample of the Rab11 with inactive PseudoJanin. The new normalized standard deviation was calculated by dividing the original calculated standard deviation for each trial — found in *Summarization of Rab7 with Active PseudoJanin Dat*a — by the average absorbance of the 1 µg/mL sample of the Rab7 with inactive PseudoJanin

Table 17. Normalization of Rab11 with Inactive PseudoJanin Data

	1 (µg/mL)	3 (µg/mL)	5 (µg/mL)	10 (µg/mL)
AVERAGE ABSORBANCE	1	1.055	1.148	1.283
STANDARD DEVIATION	.54	.60	.63	.65

Table 17 | ***Normalization of Rab11 with Inactive PseudoJanin Data.*** The table above contains the calculated normalized average absorbance and percent change in absorbance for each tested concentration of fibronectin of the Rab11 sample with inactive PseudoJanin. The normalized average absorbance was calculated by dividing the average absorbance of the 1 µg/mL, 3 µg/mL, 5 µg/mL, and 10 µg/mL of the Rab11 with inactive PseudoJanin sample by the average absorbance of the 1 µg/mL sample of the Rab11 with inactive PseudoJanin. The new normalized standard deviation was calculated by dividing the original calculated standard deviation for each trial — found in *Summarization of Rab11 with Inactive PseudoJanin Dat*a — by the average absorbance of the 1 µg/mL sample of the Rab7 with inactive PseudoJanin.

Figure 15. Comparison of Normalized Rab11 Data with Active and Inactive PseudoJanin

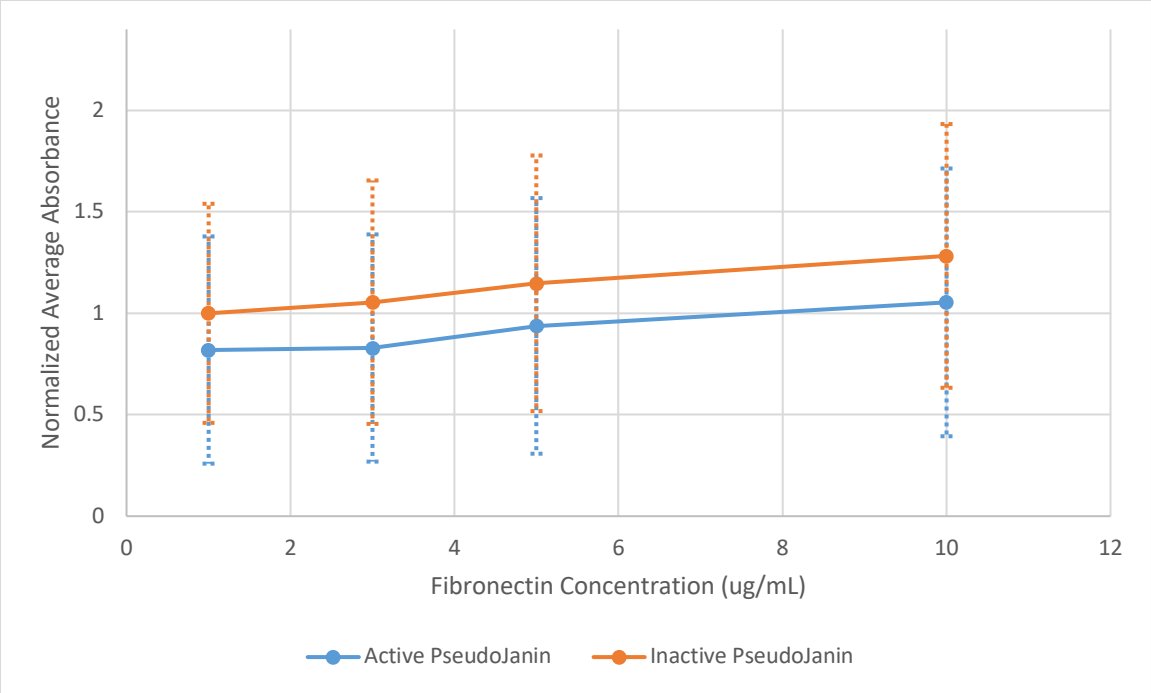

Figure 15 | ***Comparison of Normalized Rab11 Data with Active and Inactive PseudoJanin.*** The graph above depicts the calculated normalized average absorbance for both the Rab11 trial that had an active PseudoJanin, as well as the trial that had an inactive PseudoJanin. The calculated normalized average absorbance for each trial was graphed in relation to the fibronectin concentrations (1 µg/mL, 3 µg/mL, 5 µg/mL, and 10 µg/mL) for which the data was measured. The error bars represent the standard deviation of each trial and are present within *Normalization of Rab11 with Inactive PseudoJanin Data* and *Normalization of Rab11 with Active PseudoJanin Data* tables.

Table 18. Paired T-Test of Rab11 Data

Fibronectin Concentration	Two-Tailed P Value
1 µg/mL	.0447
3 µg/mL	.0170
5 µg/mL	.0415
10 µg/mL	.0328

Table 18| ***Paired T-Test of Rab11 Data.*** The table above includes the two-tailed P value calculated when comparing the normalized absorbance data for the Rab7 trials with active and inactive PseudoJanin.

Rab11 Results Summary

As can be seen in the *Comparison of Normalized Average Absorbance of Rab11 with Active and Inactive PseudoJanin,* the Rab8 sample that had a phosphate group cleaved from PIP2, the sample with active PsuedoJanin, did exhibit a lower absorbance compared to the sample that did not have a phosphate group cleaved (Inactive PseudoJanin). The Rab11 sample with the inactive PseudoJanin had a larger normalized average absorbance than the Rab11 sample with the active PseudoJanin at each measured concentration of fibronectin.

While this trend was able to be observed, it is worth also noting that there was a significant differences between the normalized average absorbance of the Rab8 samples. The paired T-test for the 1 μg/mL samples of Rab11 with and without an active PseudoJanin yielded a two-tailed P value of .0447, which is considered to be a statistically significant difference. The paired T-test for the 3 μg/mL samples of Rab11 with and without an active PseudoJanin yielded a two-tailed P value of .0170, which is considered to be a statistically significant difference. The paired T-test for the 5 μg/mL samples of Rab11 with and without an active PseudoJanin yielded a two-tailed P value of .0415, which is considered to be a statistically significant difference. The paired T-test for the 10 μg/mL samples of Rab11 with and without an active PseudoJanin yielded a two-tailed P value of .0328, which is again considered to be a statistically significant difference.

Unlike the control data and other trials, no samples exhibited the decrease in absorbance as the concentration of fibronectin increased, which was scientifically expected.

While the data did indicate that there was a significant difference between the sample with an active PseudoJanin and an inactive PseudoJanin, and there was not scientific deviations from the expected, the Rab11 samples do have a large standard deviation, although it is not as concerning as some of the other samples.

Chapter 4

Discussion

As a reminder, the goal of completing this study was to research the localization of PIP2 throughout the process of integrin and focal adhesion recycling. In order to study this, we completed an adhesion assay after transfecting HeLa cells with a synthetic Rab as well as a synthetic PseudoJanin. These two synthetic components contained a complimentary region that could dimerize in the presence of a dimerization drug rapamycin. When the Rab and PseudoJanin dimerized, the active PseudoJanin could cleave a phosphate group from PIP2, rendering the PIP2 unable to signal for the recycling of integrins. When the catalytically inactive PseudoJanin was recruited to the endosomal compartment, it was unable to cleave a phosphate from the PIP2

As mentioned in the introduction, Rab signaling proteins are associated with different endosomal compartments. Rab7 is a GTPase that is associated with late endosomes (Guerra & Bucci, 2016) and Rab8 (Henry & Sheff, 2008) and Rab11 (Wilcke *et al.*, 2000) are each associated with the recycling endosomes. In reference to the recycling endosomes, Rab8 is located at or near the recycling endosome (Henry & Sheff, 2008). Meanwhile, Rab11 is predominantly assoicated with the recycling endosome, with a degree of affiliation with the trans-Golgi network (TGN) (Wilcke *et al.*, 2000). By specifically recruiting active PseudoJanin to each of these compartments and inactivating the PIP2 within these regions, we were able to quantitatively analyze which endosome(s) contain(s) PIP2 that is critical in respect to the process of integrin recycling.

In order to provide a baseline of what a standard adhesion assay looks like, a series of control experiments were performed. The raw results from these trials are found in *Control Data* in the *Appendix*. A summary of these results is also found in *Summary of Control Data*. The data

for the control was relatively spread out with a larger standard deviation. This was a trend that was seen across all four trials, and the control data does an excellent job functioning as a baseline for absorbance and a baseline for data variability.

In addition to the control data, another control that was used throughout the trials was the inactive PseudoJanin. In order to account for variation in plating technique between trials, the lowest concentration of fibronectin of the inactive PseudoJanin functioned as a baseline that was utilized to normalize all of the trials.

While Rab8 and Rab11 both had very similar trends, the data obtained in the trial with Rab7 was very different. For starters, the Rab7 trial had the average normalized absorbance decrease as the concentration of fibronectin increased on two separate occasions. This is not a scientifically sound trend, which makes me concerned that these results were unsound. Furthermore, following completion of the statistical analysis, it became clear that the data obtained indicated that there was not a significant change between the trial that had PIP2 degraded in the late endosome versus trials that had PIP2 present in the late endosome. The average two-tailed P value of the Rab7 trials was .7767, which is again misconstrued by the fact that the pattern of the data was indistinguishable. Nonetheless, I do not feel confident claiming that the late endosome does not contain PIP2 critical to integrin recycling. Prior to making this claim, a larger sample size must be obtained and additional studies completed. The trends from this small sample size may indicate insignificance, however, a larger sample size could confirm or disprove these trends.

The Rab8 trials yielded very interesting results. Unlike the Rab7 trial, there was a distinguishable pattern, and unlike the Rab11 trial, there was no statistical significance detected. The Rab8 samples that recruited active PseudoJanin to inactivate the PIP2 in the recycling endosomes all had a lower normalized average absorbance than the samples that had no PIP2 inactivation. I feel as though this trend may indicate that there is a correlation between PIP2

presence in the recycling endosomes with efficiency of integrin recycling. Furthermore, there were slight decreases in absorbance as fibronectin concentration increased. Due to these reasons, I strongly suggest that additional trials be completed with Rab8 to study if this trend persists or if this was a coincidental pattern. The average two-tailed P value for the Rab8 trial was .5043, yet I believe that this value could shift with increased sample size and more data to further study this trend. In conclusion, the data from the Rab8 trial suggests that there may be PIP2 present within the recycling endosome that can impact the efficiency of integrin recycling, but further studies are needed before any causation can be concluded.

Unlike the other two trials, the Rab11 trials yielded results that were considered to be statistically significant. The Rab11 samples that recruited active PseudoJanin to inactivate the PIP2 in the recycling endosomes associated with the TGN all had a lower normalized average absorbance than the samples that had no PIP2 inactivation. Furthermore, all four samples had a P value $< .05$, which indicates the decrease in average normalized absorbance when the PIP2 was degraded is considered to be statistically significant. While the data indicates that statistical significance, I would suggest increasing the sample of the obtained data and completing a few more trials, as the standard deviation and variability within this data set is still large despite the low P values. In conclusion, the data from the Rab11 trial indicates that there is a strong association between the presence of PIP2 in between the samples with an active I feel as though this trend may indicate that there is a correlation between PIP2 presence in the recycling endosomes with efficiency of integrin recycling. Furthermore, there were slight decreases in absorbance as fibronectin concentration increased. Due to these reasons, I strongly suggest that additional trials be completed with Rab8 to study if this trend persists or if this was a coincidental pattern. The average two-tailed P value for the Rab8 trial was .5043, yet I believe that this value could shift with increased sample size and more data to further study this trend. In conclusion, the

data from the Rab8 trial suggests that there may be PIP2 present in the recycling endosomes associated with the TGN that impacts the efficiency with which integrins can be recycled.

Through the proceedings of this paper, the following conclusions were made: as a result of the Rab7 trials, it was found that there appears to be little to no PIP2 found within the late endosome that impact integrin recycling; as a result of the Rab8 trials, it is theorized that there is PIP2 associated with the recycling endosome that impact integrin recycling, although there is statistically no significance detected; as a result of the Rab11 trials, it was found that there appears to be PIP2 associated with the recycling endosome and TGN that has a significant impact on integrin recycling efficiency. While these conclusions are derived from the findings of these papers, more data collection could confirm or refute these results.

As for future scientific inquiry, expanding the adhesion assay model beyond the selected Rab GTPases in this study could potentially help us to understand the localization of PIP2 in other endosomal compartments. Specifically, Rab4, Rab5, Rab10, and Rab22 are all endosomal compartments that could potentially be associated with PIP2 and integrin recycling pathways. Rab4 is associated with the recycling endosome, Rab5 is associated with the early endosome, Rab10 is associated with recycling endosome and the TGN, and Rab22 is associated with the early endosome (Wandinger-Ness & Zerial, 2014). Inactivating PIP2 within each of these endosomal compartments could help to shed light on the role PIP2 plays in the process of integrin recycling and provide us with a more holistic understanding of where PIP2 is present throughout the process.

While an adhesion assay provided an effective way of measuring adhesion capabilities and quantifying recycling efficiency, an approach that assesses EMT and epithelial cell migration could provide additional context surrounding cell motility in development as well as metastasis. Researchers at UCAM have developed a protocol to quantify the ability of HeLa cells to migrate over a period a time (Liarte *et al.*, 2018). Combining their proposed migration assay with the

inactivation of PIP2 within certain endosomal compartments could provide a more holistic understanding of PIP2's role and function in biological processes such as fibrosis or tumor metastasis, helping to quantify the effects of PIP2 beyond just recycling efficiency.

Appendix

Table 19. Compilation of all Control Data

1 (µg/mL)	3 (µg/mL)	5 (µg/mL)	10 (µg/mL)
3.116	2.974	3.05	3.028
2.202	1.836	3.189	2.619
2.652	2.816	2.632	3.191
2.329	2.414	2.457	2.28
2.361	2.8843	2.224	1.924
2.439	2.414	2.29	2.796
2.71	2.843	2.565	2.966
2.03	2.227	2.323	2.624
2.746	2.017	2.932	3.048
2.367	2.47	1.905	2.862
2.903	2.329	1.822	2.314
2.051	2.694	2.131	2.584
1.721	2.466	2.635	2.874
2.848	2.55	2.443	2.466
3	2.814	2.264	2.684
2.741	2.719	2.424	2.744
2.151	2.382	2.473	3.191
2.482	3.144	2.397	2.631
2.32	2.072	2.417	2.299
2.265	2.581	2.061	2.494
2.284	2.26	2.065	2.782
2.825	2.141	2.604	
2.621	3.144	2.449	

2.473	2.515	2.643	
1.595	1.27	1.38	1.207
0.597	1.151	0.792	1.134
1.066	1.082	1.184	1.226
1.321	0.955	0.876	1.068
0.973	1.14	1.226	0.959
1.176	1.033	0.906	1.053
1.014	1.179	1.21	0.982
1.213	1.243	0.828	1.149
0.827	1.021	0.89	1.155
0.783	1.046	0.462	1.022
0.771	1.052	1.095	1.048
0.633	1.14	1.223	1.362
0.841	1.032	0.975	1.904
1.039	1.125	1	1.186
1.171	0.782	0.812	1.326
1.032	1.435	1.904	1.316
1.35	0.899	1.006	0.891
0.853	0.927	0.858	1.003
0.896	1.152	0.968	1.035
0.921	1.024	1.163	0.835
0.81	1.144	0.639	
1.036	1.347	1.053	
1.118	1.147	1.255	
1.261	1.078	1.089	
1.705	1.874	2.624	2.716
2.552	2.214	2.582	1.802
0.813	2.305	2.643	2.166
1.864	1.815	2.979	1.759
2.361	2.697	2.763	2.322
2.235	2.266	2.501	2.129
2.093	2.449	1.664	1.95
2.429	2.197	2.464	2.064
2.196	2.463	2.185	2.696
2.282	2.407	1.487	2.454
1.768	2.23	2.561	3.062
2.095	2.713		2.967

0.6419	0.9556	0.8012	0.6846
0.7521	0.5919	0.58	0.89
2.6104	2.5489	2.3239	2.6071
3.0616	3.0406	2.9046	2.7666
3.4532	2.5656	2.9035	
0.4041	0.3312	0.3687	0.4622
0.3338	0.3235	0.3029	0.5448
0.3613	0.3701	0.3008	0.6569
1.24	1.22	1.23	1.48
1.37	1.57	1.4	2.182
1.66	1.47	1.71	1.66
1.0955	1.2821	1.2719	1.6842
1.3466	1.5242	1.6834	2.5317
1.8066	1.5924	2.0017	0.8111
2.3079	2.9478	3.7361	3.6892
2.3692	2.9511	2.9532	3.1389
2.7059	3.1634	3.7299	
1.6665	2.2795	1.6601	1.6459
1.3097	0.7469	0.9409	1.1664
1.1137	1.2837	1.031	1.0209
1.1543	1.1481	1.1835	1.4532
0.395	0.3638	0.4881	0.5202
0.4385	0.5609	0.4997	0.4143
0.2211	0.362	0.691	0.7171

Table 19 | *Control Data.* The table above contains the raw data for the control trials at each concentration of fibronectin. Control trials consists of data that was obtained when transfecting cells with only one of the following: Rab7, Rab8, Rab11, PseudoJanin, or PseudoJanin Dead. The absorbance at 595 nm is listed with respect to the concentration of fibronectin for that trial. Trials are organized based off of color. This data was included to serve as a baseline for absorbance trends.

Table 20. Rab8 with Active PseudoJanin Data

1 (µg/mL)	3 (µg/mL	5 (µg/mL)	10 (µg/mL)
0.582	0.496	0.513	0.458
0.616	0.751	0.54	0.582
0.604	0.591	0.615	0.768
1.062	1.078	1.632	1.223
1.09	0.837	1.608	1.109
1.309	1.183	1.359	1.21
1.168	0.743	1.31	1.194
1.106	1.295	1.397	1.896
1.302	1.104	1.34	1.148
1.246	1.179	1.213	1.423
1.054	0.91	1.638	1.197
1.143	0.999	1.05	1.134
0.931	1.197	1.237	1.506
1.316	1.144	1.297	1.429
0.893	0.973	0.927	1.002
2.927	1.898	3.505	3.305
2.766	2.648	1.979	3.158
1.257	2.904	2.926	3.154
1.673	2.197	2.126	3.53
1.142	0.833	1.025	1.537
0.825	0.81	1.074	1.018
1.357	1.058	0.857	1.293
0.864	0.739	0.623	1.083
0.939	0.71	0.582	0.74
0.685	0.89	0.691	1.235
2.673	2.844	2.954	2.775
2.174	3.156	3.026	2.98
3.196	2.75	2.868	2.395
2.476	2.928	2.627	2.309
3.099	2.771	2.819	2.375
2.64	3.071	2.351	2.202
2.702	3.023	2.854	3.021

2.026	2.861	2.546	2.621
2.233	3.127	2.772	2.956
2.659	2.796	2.796	2.698
2.668		2.131	2.692
			2.856
1.025	1.253	0.528	1.332
0.705	0.524	0.812	1.505
0.61	0.668	1.064	0.907
0.605	1.651	1.174	1.256
0.658	0.636	1.362	1.332
0.4671	0.5026	0.6768	0.9099
0.4432	0.6564	0.6144	0.7752
0.3603	0.4971	0.5784	0.6473
0.5399	0.6917	0.6186	0.9749
0.5552	0.5286	0.8265	0.6736
0.3461	0.5192	0.559	0.6407

Table 20 | *Rab8 with Active PseudoJanin Data.* The table above contains the raw data for the Rab8 trial that had active PseudoJanin at each concentration of fibronectin. The absorbance at 595 nm is listed with respect to the concentration of fibronectin for that piece of data. Trials are organized based off of color.

Table 21. Rab8 with Inactive PseudoJanin

1 (µg/mL)	3 (µg/mL)	5 (µg/mL)	10 (µg/mL)
0.63	0.49	0.491	0.456
0.554	0.604	0.674	0.687
0.515	0.7	0.615	0.645
1.13	0.952	1.075	0.992
0.925	1.192	1.121	1.535
0.893	1.075	0.862	1.123
1.013	0.985	1.008	1.209
1.105	0.907	1.205	1.16
0.771	0.845	1.093	1.004
1.127	1.106	0.853	1.384
1.277	1.365	1.283	1.95
0.95	1.056	1.065	1.122
1.144	1.133	1.318	1.419
1.527	1.485	1.224	1.637
1.062	1.091	1.34	1.115
2.831	2.466	2.522	3.209
2.909	2.131	3.281	3.079
2.76	3.452	3.622	3.412
2.757	3.05	3.538	3.41
2.9	1.889	1.599	2.103
1.93	1.434	1.547	1.146
1.727	1.395	1.724	1.147
1.091	0.542	0.83	1.881
0.865	0.583	1.236	0.929
0.527	0.565	0.727	1.096
2.673	2.844	2.954	2.775
2.174	3.156	3.026	2.98
3.196	2.75	2.868	2.395
2.476	2.928	2.627	2.309
3.099	2.771	2.819	2.375
2.64	3.071	2.351	2.202
2.702	3.023	2.854	3.021
2.026	2.861	2.546	2.621

2.233	3.127	2.772	2.956
2.659	2.796	2.796	2.698
2.668		2.131	2.692
			2.856
0.3508	0.335	0.4789	0.8006
0.3929	0.3131	0.4344	0.6166
0.4397	0.3205	0.335	0.5492
0.5948	0.5584	0.5359	0.8482
0.4429	0.4206	0.5598	0.5681
	0.5177	0.534	0.5581

Table 21 | *Rab8 with Inactive PseudoJanin Data.* The table above contains the raw data for the Rab8 trial that had inactive PseudoJanin at each concentration of fibronectin. The absorbance at 595 nm is listed with respect to the concentration of fibronectin for that piece of data. Trials are organized based off of color.

Table 22. Rab7 with Active PseudoJanin Data

1 (µg/mL)	3 (µg/mL)	5 (µg/mL)	10
0.975	0.73	0.827	0.833
0.857	1.039	0.717	0.788
0.636	0.646	0.606	0.642
0.916	0.983	0.979	1.298
0.813	0.701	0.988	0.966
0.766	0.854	0.806	0.9
0.778	0.787	0.72	0.991
0.803	0.56	0.953	1.408
0.794	0.611	0.845	1.179
0.676	1.156	1.178	0.859
0.731	0.885	0.867	1.088
0.772	0.959	0.774	1.149
0.604	1.142	0.614	0.852
0.681	0.694	0.936	1.088
0.548	0.638	0.763	1.098
1.751	2.551	2.133	3.446
3.041	1.882	2.702	3.711
1.929	2.592	3.612	2.218
2.399	3.116	MAX	3.544

Table 22 | *Rab7 with Active PseudoJanin Data.* The table above contains the raw data for the Rab7 trial that had active PseudoJanin at each concentration of fibronectin. The absorbance at 595 nm is listed with respect to the concentration of fibronectin for that piece of data. Trials are organized based off of color.

Table 23. Rab7 with Inactive PsuedoJanin

1 (µg/mL)	3 (µg/mL)	5 (µg/mL)	10 (µg/mL)
0.589	0.525	0.597	0.74
0.624	0.597	0.559	0.501
0.57	0.559	0.633	0.756
0.821	1.103	0.805	0.877
0.939	0.677	0.986	0.817
0.684	1.043	0.674	1.274
0.805	0.933	0.869	1.241
0.752	0.669	1.011	0.811
0.79	0.659	0.969	1.581
0.951	1.604	1.037	1.053
0.801	0.648	1.075	1.012
1.005	1.072	0.996	1.208
1.097	0.952	0.998	1.135
1.198	0.964	0.987	1.411
0.887	0.985	1.45	1.622
1.077	2.047	2.338	4.009
2.79	2.142	2.945	3.314
2.695	2.686	3.741	2.022
3.424	2.553	3.752	2.497

Table 23 | *Rab7 with Inactive PseudoJanin Data.* The table above contains the raw data for the Rab7 trial that had inactive PseudoJanin at each concentration of fibronectin. The absorbance at 595 nm is listed with respect to the concentration of fibronectin for that piece of data. Trials are organized based off of color.

Table 24. Rab11 with Active PseudoJanin

1 (µg/mL)	3 (µg/mL)	5 (µg/mL)	10 (µg/mL)
0.616	0.61	0.475	0.45
0.569	0.819	1.056	0.638
0.535	0.655	0.568	0.688
0.693	0.74	0.678	0.667
0.668	0.645	0.742	0.512
0.58	0.805	0.612	0.454
0.665	0.654	1.057	0.688
0.773	0.457	0.993	0.653
0.711	1.178	0.713	0.776
1.205	0.94	0.691	0.875
0.829	0.83	0.85	0.536
0.943	0.535	0.79	2
0.672	0.793	0.515	1.662
[redacted]	0.825	0.82	0.792
[redacted]	0.829	0.638	0.633
2.596	3.742	3.168	3.72
3.097	1.633	2.129	3.308
3.169	1.622	3.701	3.617
2.126	1.814	3.357	3.202
0.624	0.675	0.703	1.058
0.764	0.564	0.623	0.839
0.439	0.606	0.801	1.041
0.622	0.712	0.754	1.277
0.592	0.52	0.576	0.812
0.584	0.693	0.799	1.496
0.778	1.075	1.577	2.032
0.853	1.224	1.651	2.235
1.323	1.218	1.222	2.1
0.783	0.77	1.106	1.509
0.99	1.071	1.001	1.368
0.807	0.998	1.517	1.697
0.955	0.995	1.359	1.565
0.871	1.116	1.346	1.757

0.791	0.753	1.377	1.78
0.855	1.324	1.03	2.846
0.758	0.7	1.455	3.111
1.292	0.609	1.261	2.031
2.672	2.468	3.074	2.946
2.654	2.67	3.004	2.89
2.704	3.153	2.889	3.454
2.792	2.61	3.003	2.784
2.765	2.869	3.147	2.999
2.215	MAX	3.116	3.061
2.957	2.765	3.363	MAX
2.676	2.821	3.035	3
2.949	3.127	3.081	2.723
2.837	3.041	2.986	2.872
2.355	2.558	2.912	2.922
	3.331	2.853	3.396
0.639	0.97	0.908	0.943
0.836	1.108	0.972	1.67
0.757	1.108	1.161	1.137
1.018	1.068	0.878	0.92
0.811	1.033	1.108	0.83
0.776	0.836	1.225	1.231
1.062	1.18	1.257	0.84
1.037	1.313	0.936	1
1.349	1.236	1.449	1.093
0.846	0.09	0.948	0.979
0.891	1.069	1.243	1.092
0.771	0.667	1.258	1.418
0.958	1.328	0.923	1.058
0.839	0.556	0.965	1.381
0.916	1.015	1.502	1.363
0.8	1.25	1.03	1.353
1.015	0.741	1.087	1.448
0.96	1.024	1.447	1.083
0.957	1.465	0.789	1.28
0.951	0.59	0.923	0.945
1.045	1.074	0.977	1.285

0.876	1.255	0.965	1.255
0.697	0.692	1.218	0.789
0.668	0.645	0.742	0.512
0.58	0.805	0.612	0.454
0.665	0.654	1.057	0.688
0.773	0.457	0.993	0.653
0.711	1.178	0.713	0.776
1.205	0.94	0.691	0.875
0.829	0.83	0.85	0.536
0.943	0.535	0.79	2
0.672	0.793	0.515	1.662
	0.825	0.82	0.792
	0.829	0.638	0.633
0.2981	0.6114	0.392	0.5566
0.22	0.2466	0.3936	0.5977
0.2089	0.3789	0.4477	0.5368
0.3605	0.553	0.6074	0.6312
	0.3614	0.5624	0.7435
		0.1996	

Table 24 | *Rab11 with Active PseudoJanin Data.* The table above contains the raw data for the Rab11 trial that had active PseudoJanin at each concentration of fibronectin. The absorbance at 595 nm is listed with respect to the concentration of fibronectin for that piece of data. Trials are organized based off of color.

Table 25. Rab11 with Inactive PseudoJanin

1 (µg/mL)	3 (µg/mL)	5 (µg/mL)	10 (µg/mL)
0.95	0.9	2.267	0.768
0.696	0.67	0.592	0.903
0.621	0.645	0.675	0.626
0.743	0.823	0.775	0.774
1.439	0.898	1.258	1.259
1.257	1.23	1.068	1.68
1.225	1.233	1.206	2.186
1.213	1.543	1.136	1.106
1.55	1.563	1.323	1.117
1.474	1.899	1.441	1.002
1.294	1.28	2.035	0.934
1.508	2.123	1.37	1.003
1.462	1.324	1.259	1.62
1.689	1.06	1.527	1.238
1.371	1.177	1.511	2.576
1.2	2.039	0.942	1.528
2.055	2.848	1.447	3.555
1.622	1.795	3.22	3.498
2.726	1.776	3.449	3.217
1.52	1.684	3.187	MAX
1.13	0.98	1.099	1.065
1.109	1.021	1.205	1.442
1.428	1.893	1.009	1.341
0.808	0.647	0.77	0.89
0.75	0.61	0.755	0.709
0.602	0.686	0.927	1.044
0.981	0.832	0.659	2.396
0.755	0.691	0.982	2.227
0.718	0.661	0.799	1.522
0.911	1.2	1.075	1.71
0.798	0.876	0.953	1.875
1.008	0.81	1.202	2.066
0.923	0.996	1.284	1.928

0.983	0.926	1.187	1.305
0.75	0.798	1.278	1.626
0.899	1.25	1.518	2.077
0.899	1.059	1.421	1.973
0.84	0.822	1.562	2.382
3.3	3.22	3.273	3.033
3.26	3.307	3.335	3.132
3.22	3.445	3.29	3.203
2.642	2.783	3.231	MAX
2.687	3.023	3.035	3.183
2.187	3.038	3.002	3.511
2.715	2.425	2.665	2.943
2.183	2.556	3.005	3.352
2.319	2.744	2.918	3.463
2.517	2.775	2.631	3.108
2.99	2.581	2.79	2.978
2.227	2.831	3.193	3.377
1.439	0.898	1.258	1.259
1.257	1.23	1.068	1.68
1.225	1.233	1.206	2.186
1.213	1.543	1.136	1.106
1.55	1.563	1.323	1.117
1.474	1.899	1.441	1.002
1.294	1.28	2.035	0.934
1.508	2.123	1.37	1
1.462	1.324	1.259	1.62
1.689	1.06	1.527	1.238
1.371	1.177	1.511	2.576
1.2	2.039	0.942	1.528
0.2591	0.5181	0.4804	1.0334
0.3432	0.3439	0.7194	0.9651
0.2992	0.3163	0.9623	0.5849
0.3324	0.5637	0.7278	0.9243
0.2497	0.4103	0.5757	0.9183
0.4417	0.4098		0.7023

Table 25 | ***Rab11 with Inactive PseudoJanin Data.*** The table above contains the raw data for the Rab11 trial that had inactive PseudoJanin at each concentration of fibronectin. The absorbance at

595 nm is listed with respect to the concentration of fibronectin for that piece of data. Trials are organized based off of color.

BIBLIOGRAPHY

Adil, M. S.; Narayanan, S. P.; Somanath, P. R. Cell-cell junctions: structure and regulation in physiology and pathology. *Tissue Barriers* **2020**, *9* (1), 1848212. https://doi.org/10.1080/21688370.2020.1848212.

Alberts B, Johnson A, Lewis J, et al. Molecular Biology of the Cell. 4th edition. New York: Garland Science; 2002. Integrins. Available from: https://www.ncbi.nlm.nih.gov/books/NBK26867/.

Das, M.; Ithychanda, S. S.; Qin, J.; Plow, E. F. Mechanisms of talin-dependent integrin signaling and crosstalk. *Biochimica Et Biophysica Acta (BBA) - Biomembranes* **2014**, *1838* (2), 579–588. https://doi.org/10.1016/j.bbamem.2013.07.017.

De Franceschi, N.; Hamidi, H.; Alanko, J.; Sahgal, P.; Ivaska, J. Integrin traffic – the update. *Journal of Cell Science* **2015**. https://doi.org/10.1242/jcs.161653.

Guerra, F.; Bucci, C. Multiple roles of the small GTPase RAB7. *Cells* **2016**, *5* (3), 34. https://doi.org/10.3390/cells5030034.

Hamidi, H.; Ivaska, J. Every step of the way: integrins in cancer progression and metastasis. *Nature Reviews Cancer* **2018**, *18* (9), 533–548. https://doi.org/10.1038/s41568-018-0038-z.

Henry, L.; Sheff, D. RAB8 regulates basolateral secretory, but not recycling, traffic at the recycling endosome. *Molecular Biology of the Cell* **2008**, *19* (5), 2059–2068. https://doi.org/10.1091/mbc.e07-09-0902.

Humphries, J. D.; Wang, P.; Streuli, C.; Geiger, B.; Ballestrem, C. Vinculin controls focal adhesion formation by direct interactions with talin and actin. *Journal of Cell Biology* **2007**, *179* (5), 1043–1057. https://doi.org/10.1083/jcb.200703036.

Kalluri, R.; Weinberg, R. A. The basics of epithelial-mesenchymal transition. *Journal of Clinical Investigation* **2009**, *119* (6), 1420–1428. https://doi.org/10.1172/jci39104.

Lai, T.-Y.; Cao, J.; Ou-Yang, P.; Tsai, C. F.; Lin, C.-C.; Chen, C.-C.; Tsai, M.; Lee, C.-Y. Different methods of detaching adherent cells and their effects on the cell surface expression of Fas receptor and Fas ligand. *Scientific Reports* **2022**, *12* (1). https://doi.org/10.1038/s41598-022-09605-y.

Liarte, S.; Bernabé-García, Á.; Armero-Barranco, D.; Nicolás, F. Microscopy Based Methods for the Assessment of Epithelial Cell Migration During In Vitro Wound Healing. *Journal of Visualized Experiments* **2018**, No. 131. https://doi.org/10.3791/56799.

Loh, C.-Y.; Chai, J. Y.; Tang, T.; Wong, W. F.; Sethi, G.; Shanmugam, M. K.; Chong, P. P.; Looi, C. Y. The E-Cadherin and N-Cadherin Switch in Epithelial-to-Mesenchymal Transition: signaling, therapeutic implications, and challenges. *Cells* **2019**, *8* (10), 1118. https://doi.org/10.3390/cells8101118.

Mandal, K. Review of PIP2 in Cellular Signaling, Functions and Diseases. *International Journal of Molecular Sciences* **2020**, *21* (21), 8342. https://doi.org/10.3390/ijms21218342.

Martínez-Arroyo, O.; Selma-Soriano, E.; Ortega, A.; Cortés, R.; Redón, J. Small RAB GTPases in intracellular vesicle trafficking: the case of RAB3A/Raphillin-3A complex in the kidney. *International Journal of Molecular Sciences* **2021**, *22* (14), 7679. https://doi.org/10.3390/ijms22147679.

Nelson, W. J. Remodeling Epithelial cell Organization: Transitions between Front-Rear and Apical-Basal polarity. *Cold Spring Harbor Perspectives in Biology* **2009**, *1* (1), a000513. https://doi.org/10.1101/cshperspect.a000513.

Oh, S. H.; Santy, L. C. Differential Effects of Cytohesins 2 and 3 on β1 Integrin Recycling. *Journal of Biological Chemistry* **2010**, *285* (19), 14610–14616. https://doi.org/10.1074/jbc.m109.043935.

Oh, S. H.; Santy, L. C. Phosphoinositide specificity determines which cytohesins regulate β1 integrin recycling. *Journal of Cell Science* **2012**. https://doi.org/10.1242/jcs.101683.

Ridley, A. J.; Schwartz, M. A.; Burridge, K.; Firtel, R. A.; Ginsberg, M. H.; Borisy, G. G.; Parsons, J. T.; Horwitz, A. R. Cell Migration: Integrating Signals from Front to Back. *Science* **2003**, *302* (5651), 1704–1709. https://doi.org/10.1126/science.1092053.

Singh, N.; Reyes-Ordoñez, A.; Compagnone, M. A.; Moreno, J.; Leslie, B. J.; Ha, T.; Chen, J. Redefining the specificity of phosphoinositide-binding by human PH domain-containing proteins. *Nature Communications* **2021**, *12* (1). https://doi.org/10.1038/s41467-021-24639-y.

Sohn, M.; Korzeniowski, M.; Zewe, J. P.; Wills, R. C.; Hammond, G.; Humpolíčková, J.; Vrzal, L.; Chalupská, D.; Veverka, V.; Fairn, G. D.; Bouřa, E.; Balla, T. PI(4,5)P2 controls plasma membrane PI4P and PS levels via ORP5/8 recruitment to ER–PM contact sites. *Journal of Cell Biology* **2018**, *217* (5), 1797–1813. https://doi.org/10.1083/jcb.201710095.

Thapa, N.; Anderson, R. A. PIP2 signaling, an integrator of cell polarity and vesicle trafficking in directionally migrating cells. *Cell Adhesion & Migration* **2012**, *6* (5), 409–412. https://doi.org/10.4161/cam.21192.

Wandinger-Ness, A.; Zerial, M. RAB proteins and the compartmentalization of the endosomal system. *Cold Spring Harbor Perspectives in Biology* **2014**, *6* (11), a022616. https://doi.org/10.1101/cshperspect.a022616.

Wang, Z.-W.; Hu, X.; Ye, M.; Lin, M.; Chu, M.; Shen, X. NEDD4 E3 ligase: Functions and mechanism in human cancer. *Seminars in Cancer Biology* **2020**, *67*, 92–101. https://doi.org/10.1016/j.semcancer.2020.03.006.

Wilcke, M.; Johannes, L.; Galli, T.; Mayau, V.; Goud, B.; Salamero, J. Rab11 Regulates the Compartmentalization of Early Endosomes Required for Efficient Transport from Early Endosomes to the Trans-Golgi Network. *Journal of Cell Biology* **2000**, *151* (6), 1207–1220. https://doi.org/10.1083/jcb.151.6.1207.

Yang, J.; Weinberg, R. A. Epithelial-Mesenchymal transition: at the crossroads of development and tumor metastasis. *Developmental Cell* **2008**, *14* (6), 818–829. https://doi.org/10.1016/j.devcel.2008.05.009.

Zerial, M.; McBride, H. M. Rab proteins as membrane organizers. *Nature Reviews Molecular Cell Biology* **2001**, *2* (2), 107–117. https://doi.org/10.1038/35052055.